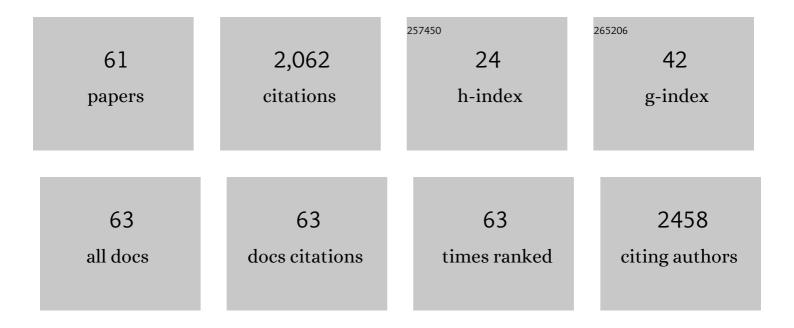
List of Publications by Year in descending order

Source: https://exaly.com/author-pdf/838585/publications.pdf Version: 2024-02-01



#	Article	IF	CITATIONS
1	Novel SnO2@ZnO hierarchical nanostructures for highly sensitive and selective NO2 gas sensing. Sensors and Actuators B: Chemical, 2018, 257, 714-727.	7.8	157
2	Bismuth Vacancy-Tuned Bismuth Oxybromide Ultrathin Nanosheets toward Photocatalytic CO ₂ Reduction. ACS Applied Materials & Interfaces, 2019, 11, 30786-30792.	8.0	140
3	Phase-controllable growth of ultrathin 2D magnetic FeTe crystals. Nature Communications, 2020, 11, 3729.	12.8	120
4	Cobalt nitride as a novel cocatalyst to boost photocatalytic CO2 reduction. Nano Energy, 2021, 79, 105429.	16.0	117
5	Amorphizing noble metal chalcogenide catalysts at the single-layer limit towards hydrogen production. Nature Catalysis, 2022, 5, 212-221.	34.4	113
6	Carbon Microtube Aerogel Derived from Kapok Fiber: An Efficient and Recyclable Sorbent for Oils and Organic Solvents. ACS Nano, 2020, 14, 595-602.	14.6	104
7	Ultraâ€Robust and Extensible Fibrous Mechanical Sensors for Wearable Smart Healthcare. Advanced Materials, 2022, 34, e2107511.	21.0	83
8	Strain-Engineering of Bi ₁₂ O ₁₇ Br ₂ Nanotubes for Boosting Photocatalytic CO ₂ Reduction. , 2020, 2, 1025-1032.		82
9	Machine learning-guided synthesis of advanced inorganic materials. Materials Today, 2020, 41, 72-80.	14.2	70
10	First-principles calculations and experimental investigation on SnO2@ZnO heterojunction photocatalyst with enhanced photocatalytic performance. Journal of Colloid and Interface Science, 2019, 553, 613-621.	9.4	67
11	Oxygen vacancy mediated bismuth stannate ultra-small nanoparticle towards photocatalytic CO2-to-CO conversion. Applied Catalysis B: Environmental, 2020, 276, 119156.	20.2	59
12	Recent progress of flexible electronics by 2D transition metal dichalcogenides. Nano Research, 2022, 15, 2413-2432.	10.4	58
13	Enhanced radar and infrared compatible stealth properties in hierarchical SnO2@ZnO nanostructures. Ceramics International, 2017, 43, 3443-3447.	4.8	52
14	Single CdS Nanorod for High Responsivity UV–Visible Photodetector. Advanced Optical Materials, 2017, 5, 1700159.	7.3	47
15	Microwave-assistant hydrothermal synthesis of SnO 2 @ZnO hierarchical nanostructures enhanced photocatalytic performance under visible light irradiation. Materials Research Bulletin, 2018, 106, 74-80.	5.2	38
16	Enhanced visible light photocatalytic performances of few-layer MoS2@TiO2 hollow spheres heterostructures. Materials Research Bulletin, 2020, 130, 110936.	5.2	37
17	Optogenetics inspired transition metal dichalcogenide neuristors for in-memory deep recurrent neural networks. Nature Communications, 2020, 11, 3211.	12.8	36
18	Spaceâ€confined microwave synthesis of ternaryâ€layered BiOCl crystals with highâ€performance ultraviolet photodetection. InformaÄnÃ-Materiály, 2020, 2, 593-600.	17.3	32

#	Article	IF	CITATIONS
19	Construction of hierarchical SnO2@Fe3O4 nanostructures for efficient microwave absorption. Journal of Magnetism and Magnetic Materials, 2020, 498, 166224.	2.3	30
20	Machine Learning Driven Synthesis of Few-Layered WTe ₂ with Geometrical Control. Journal of the American Chemical Society, 2021, 143, 18103-18113.	13.7	30
21	Construction of highly ordered ZnO microrod@SnO2 nanowire heterojunction hybrid with a test-tube brush-like structure for high performance lithium-ion batteries: experimental and theoretical study. Electrochimica Acta, 2020, 330, 135312.	5.2	29
22	Recent Advances in Synthesis and Study of 2D Twisted Transition Metal Dichalcogenide Bilayers. Small Structures, 2021, 2, 2000153.	12.0	29
23	Terahertz Surface Emission from MoSe ₂ at the Monolayer Limit. ACS Applied Materials & Interfaces, 2020, 12, 48161-48169.	8.0	28
24	Reversible and high-capacity SnO 2 /carbon cloth composite electrode materials prepared by magnetron sputtering for Li-ion batteries. Materials Letters, 2017, 190, 56-59.	2.6	26
25	Facile synthesis of nano-MoS 2 and its visible light photocatalytic property. Materials Research Bulletin, 2017, 87, 119-122.	5.2	26
26	Preparation and electrochemical performance of bramble-like ZnO array as anode materials for lithium-ion batteries. Journal of Nanoparticle Research, 2015, 17, 1.	1.9	25
27	2D Cairo Pentagonal PdPS: Air‣table Anisotropic Ternary Semiconductor with High Optoelectronic Performance. Advanced Functional Materials, 2022, 32, .	14.9	25
28	New strategy towards the assembly of hierarchical heterostructures of SnO ₂ /ZnO for NO ₂ detection at a ppb level. Inorganic Chemistry Frontiers, 2019, 6, 2801-2809.	6.0	24
29	MoO ₃ –MoS ₂ vertical heterostructures synthesized via one-step CVD process for optoelectronics. 2D Materials, 2021, 8, 035036.	4.4	24
30	DFT study of the effect of BN pair doping on the electronic and optical properties of graphyne nanosheets. Journal of Materials Science, 2017, 52, 10294-10307.	3.7	21
31	First-principles study of B or Al-doping effect on the structural, electronic structure and magnetic properties of Î ³ -graphyne. Computational Materials Science, 2015, 108, 147-152.	3.0	20
32	Effect of single vacancy on the structural, electronic structure and magnetic properties of monolayer graphyne by first-principles. Materials Chemistry and Physics, 2016, 182, 439-444.	4.0	18
33	Giant and Anisotropic Nonlinear Optical Responses of 1D van der Waals Material Tellurium. Advanced Optical Materials, 2020, 8, 2001273.	7.3	17
34	Shape-controlled and stable hollow frame structures of SnO and their highly sensitive NO2 gas sensing. Sensors and Actuators B: Chemical, 2021, 340, 129940.	7.8	17
35	Ultrasensitive NO2 gas sensor based on Sb-doped SnO2 covered ZnO nano-heterojunction. Journal of Materials Science, 2021, 56, 7348-7356.	3.7	17
36	Tunable band gap of graphyne-based homo- and hetero-structures by stacking sequences, strain and electric field. Physical Chemistry Chemical Physics, 2018, 20, 26934-26946.	2.8	16

#	Article	IF	CITATIONS
37	Highly Sensitive Flexible Temperature Sensor Made Using PEDOT:PSS/PANI. ACS Applied Polymer Materials, 2022, 4, 766-772.	4.4	16
38	Direct growth of single-metal-atom chains. , 2022, 1, 245-253.		16
39	PdPSe: Componentâ€Fusionâ€Based Topology Designer of Twoâ€Dimensional Semiconductor. Advanced Functional Materials, 2021, 31, 2102943.	14.9	15
40	A hierarchical sandwich-structured MoS2/SnO2/CC heterostructure for high photocatalysis performance. Materials Letters, 2019, 236, 697-701.	2.6	13
41	Hydrothermal synthesis and photoluminescence properties of SnO2 nanowire array and pinecone-like nanoparticles on ITO substrate. Materials Letters, 2016, 165, 243-246.	2.6	12
42	Effect of Sb-doping on the morphology and the infrared emissivity of peony-like SnO2 microspheres. Integrated Ferroelectrics, 2018, 191, 1-7.	0.7	12
43	Facile synthesis of oil adsorbent carbon microtubes by pyrolysis of plant tissues. Journal of Materials Science, 2019, 54, 9352-9361.	3.7	12
44	Two-step chemical vapor deposition synthesis of NiTe ₂ -MoS ₂ vertical junctions with improved MoS ₂ transistor performance. Nanotechnology, 2021, 32, 235204.	2.6	12
45	Programmable patterned MoS2 film by direct laser writing for health-related signals monitoring. IScience, 2021, 24, 103313.	4.1	12
46	Inversion symmetry broken in 2H phase vanadium-doped molybdenum disulfide. Nanoscale, 2021, 13, 18103-18111.	5.6	11
47	Synthesis, growth mechanism, and photoluminescence property of hierarchical SnO2 nanoflower-rod arrays: an experimental and first principles study. Journal of Materials Science, 2016, 51, 9613-9624.	3.7	10
48	Ingenious design of Cu/Ni substrate for hot filament chemical vapor deposition growth of high quality graphene films. Diamond and Related Materials, 2017, 72, 7-12.	3.9	9
49	Inventive design of Cu/SiO2 substrate for chemical vapor deposition preparation of dense carbon nanofibers. Diamond and Related Materials, 2018, 89, 174-179.	3.9	9
50	In-situ growth of W18O49@carbon clothes for flexible-easy-recycled photocatalysts with high performance. Materials Letters, 2018, 230, 224-227.	2.6	9
51	Enhancing the cycling stability of Na-ion batteries by bonding MoS2 on assembled carbon-based materials. Nano Materials Science, 2019, 1, 310-317.	8.8	9
52	One-pot solvothermal preparation of mesoporous Cu(II)Porphyrin-TiO ₂ composites with enhanced photocatalytic activity and stability. Inorganic and Nano-Metal Chemistry, 2017, 47, 783-787.	1.6	8
53	Pressure induced photoluminescence modulation in a wide range and synthesis of monodispersed ternary AgCuS nanocrystal based on Ag ₂ S nanocrystals. Nanoscale, 2018, 10, 2577-2587.	5.6	7
54	Blue-violet emission of silicon carbonitride thin films prepared by sputtering and annealing treatment. Applied Surface Science, 2021, 546, 149121.	6.1	7

#	Article	IF	CITATIONS
55	Controlled growth of ultrathin ferromagnetic βâ€MnSe semiconductor. SmartMat, 2022, 3, 482-490.	10.7	7
56	Solid-Ionic Memory in a van der Waals Heterostructure. ACS Nano, 2022, 16, 221-231.	14.6	6
57	Sizeâ€Đependent Activity of Ironâ€Nickel Oxynitride towards Electrocatalytic Oxygen Evolution. ChemNanoMat, 2019, 5, 883-887.	2.8	5
58	Study on photoelectricity properties of SiCN thin films prepared by magnetron sputtering. Journal of Materials Research and Technology, 2021, 15, 460-467.	5.8	5
59	A novel preparation method for uniform large-area graphene films on Ni@Cu substrate. Materials Today Communications, 2019, 21, 100607.	1.9	1
60	Physical Vapor Deposition Growth of Ultrathin Molybdenum Dioxide Nanosheets with Excellent Conductivity. Advanced Engineering Materials, 0, , 2101358.	3.5	1
61	Effect of Sn/Zn ratio on structure and photoluminescence properties of SnO ₂ @ZnO composites. Integrated Ferroelectrics, 2018, 189, 189-196.	0.7	Ο